



## Variability in Deep Western Boundary Current transports: Preliminary results from 26.5°N in the Atlantic

Christopher S. Meinen,<sup>1</sup> Molly O. Baringer,<sup>1</sup> and Silvia L. Garzoli<sup>1</sup>

Received 19 May 2006; revised 31 July 2006; accepted 9 August 2006; published 13 September 2006.

[1] Transport fluctuations of the deep limb of the Meridional Overturning Circulation (MOC) near the western boundary are presented from a line of inverted echo sounders, bottom pressure sensors, and a deep current meter east of Abaco Island, Bahamas, at 26.5°N from September 2004 through September 2005. The mean southward flow between 800 dbar and 4800 dbar was  $39 \times 10^6 \text{ m}^3 \text{ s}^{-1}$ , with a northward recirculation of  $28 \times 10^6 \text{ m}^3 \text{ s}^{-1}$ , leaving a net southward flow of  $11 \times 10^6 \text{ m}^3 \text{ s}^{-1}$  as the through-flow of the Deep Western Boundary Current (DWBC). The mean southward DWBC flow essentially equals previous values that were measured at the same location by arrays of current meters deployed from 1986 to 1992. DWBC transport spectra indicate that barotropic and baroclinic changes have very similar energy levels at most periods less than 10 days and that barotropic changes dominate at periods of 10–80 days. **Citation:** Meinen, C. S., M. O. Baringer, and S. L. Garzoli (2006), Variability in Deep Western Boundary Current transports: Preliminary results from 26.5°N in the Atlantic, *Geophys. Res. Lett.*, 33, L17610, doi:10.1029/2006GL026965.

### 1. Introduction

[2] Numerical climate models have shown a significant correlation between the Atlantic Meridional Overturning Circulation (MOC) and surface air-temperatures globally [e.g., Vellinga and Wood, 2002; Stouffer et al., 2006], emphasizing the importance of the MOC for climate. Recognition of this importance is not new, with significant efforts at quantifying components of the MOC at 26.5°N beginning in the mid-1980s [Lee et al., 1990, 1996; Baringer and Larsen, 2001]. The U.S. National Oceanic and Atmospheric Administration (NOAA) began monitoring the Florida Current, believed to carry the majority of the upper limb of the MOC, in 1982 using a submarine cable across the Florida Straits near 27°N [Larsen and Sanford, 1985; Larsen, 1992] (see Figure 1). In 1985 NOAA expanded the program offshore of the Bahamas Islands at 26.5°N to measure the structure and transport of the southward flowing Deep Western Boundary Current (DWBC) and the northward flowing Antilles Current via hydrographic sections and occasionally with current meter mooring arrays [e.g., Lee et al., 1990, 1996; Molinari et al., 1992; Hacker et al., 1996; Johns et al., 2005]. In 1996 NOAA continued to expand its program by including time series observations of the DWBC using inverted echo

sounders (IESs) for a one-year pilot study. Using the one year of data from this pilot experiment, Meinen et al. [2004] demonstrated that the combination of bottom pressure and IES data could determine the DWBC transport at a similar level of accuracy as a traditional picket fence array of current meter moorings at a fraction of the cost (see Figure 2). Beginning in September 2004 the NOAA IES array was redeployed and expanded to include bottom pressure sensors and a deep current meter in what is intended to be a long-term monitoring system similar to the cable-based Florida Current measurements.

[3] The NOAA Western Boundary Time Series program encompasses both the Florida Current monitoring program (via hydrographic section and submarine cable), routine hydrographic sections across the DWBC, and the new IES-based transport monitoring system. The program also contributes to an international program designed to monitor the complete heat flux across 26°N by spanning the whole Atlantic with tall moorings; the U.S. component of the international program is called the Meridional Overturning Circulation Heat-transport Array (MOCHA), while the United Kingdom component is part of the RAPID Climate Change program [Srokosz, 2003; Hirschi et al., 2003; Baehr et al., 2004]. This paper highlights the preliminary results from the NOAA IES array for the first twelve months of the DWBC time series transport array from September 2004 through September 2005.

### 2. Methods

[4] The September 2004 deployment consisted of three different types of IES; one basic IES, three IESs additionally equipped with a pressure sensor (PIES), and one IES with both a pressure sensor and a current meter 50 m above the bottom connected via cable (C-PIES). In March 2006 the basic IES was replaced with a PIES, and all instruments are planned to remain in place indefinitely (with four year deployments) collecting data as part of NOAA's sustained Ocean Observing System. Data is downloaded acoustically from the instruments by a passing research vessel approximately every six months. Site names A–E for the PIES and C-PIES moorings are shown in Figure 1, which also shows a mean meridional velocity section based on Pegasus and LADCP data obtained during earlier studies in the 1980s [e.g., Molinari et al., 1992; Hacker et al., 1996]. The mean Pegasus/LADCP velocity section in Figure 1 is shown simply to illustrate where the IES sites are relative to the basic circulation features, recognizing that all of these features move and change in time.

[5] Travel time measurements from PIES and bottom pressure data have been combined to estimate absolute velocity profiles and transports at a number of locations,

<sup>1</sup>Atlantic Oceanographic and Meteorological Laboratory, Miami, Florida, USA.

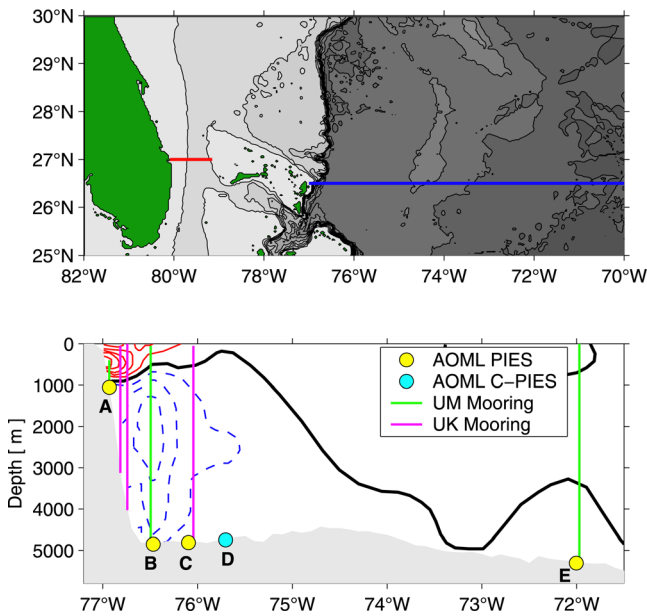


**Figure 1.** (top) Location of the NOAA Florida Current cable (red line) and the section along which the IESs are deployed and where annual NOAA hydrographic cruises are completed (blue line). (bottom) Locations of the NOAA IESs across the continental shelf and slope. Also shown are the locations of the tall MOCHA-RAPID moorings. Contours are an average of Pegasus and LADCP data obtained in the late 1980s and early 1990s; contour interval is  $5 \text{ cm s}^{-1}$ , with blue contours indicating southward flow and red contours indicating northward flow; black line indicates zero flow.

for example the North Atlantic Current [Meinen and Watts, 2000]. The details of how bottom pressure, hydrography, and IES data are combined to produce time series sections of absolute velocities are found elsewhere [Meinen and Watts, 2000; Watts et al., 2001a; Meinen et al., 2004]. In brief, hydrography (both contemporaneous and historical) from the region of interest is used to develop look-up tables of temperature ( $T$ ), salinity ( $S$ ), and specific volume anomaly ( $\delta$ ) as functions of pressure and acoustical travel time ( $\tau$ ) [Meinen and Watts, 2000]. IES measurements of  $\tau$  can be combined with these look-up tables to yield time series of full water column profiles of  $T$ ,  $S$ , and  $\delta$  at each IES site along with hydrography-based error estimates for each of these quantities. Profiles of  $\delta$  can be vertically integrated to give geopotential height anomaly profiles ( $\Delta\Phi$ ), and differences in  $\Delta\Phi$  profiles from neighboring IES sites provide geostrophic velocity profiles relative to an assumed level of no motion. Bottom pressure measurements can be differenced from neighboring sites to give absolute velocity variability near the bottom. However, the time-mean bottom velocity cannot be so-determined due to the so-called “leveling” problem wherein bottom depth changes cannot be distinguished from deep geostrophic pressure gradients [e.g., Watts et al., 2001b]. If a time-mean bottom-velocity estimate is available (such as from the historical current meter records at  $26.5^\circ\text{N}$ , which were recently compiled by Bryden et al., 2005a) then this mean can be added to the time-varying bottom velocities determined from the bottom

pressure records and the resulting absolute bottom velocities can be used to reference the IES-derived relative velocity profiles to produce absolute velocity profiles between pairs of PIES.

[6] Meinen et al. [2004] provides a detailed appendix on the accuracy of the transports estimated via the methods described above and compared those transports to volume transport estimates from a ‘picket fence’ current meter array (Figure 2). Briefly, hydrographic scatter can provide an estimate of the accuracy of the geostrophic relative velocities determined from the IES travel time data. This error, which includes scatter due to higher vertical modes as well as trends in hydrographic properties, was estimated to be about  $3 \text{ Sv}$  ( $1 \text{ Sv} = 10^6 \text{ m}^3 \text{ s}^{-1}$ ) for 5-day running averaged DWBC transport data. The high precision pressure gauges used in the PIES are accurate to within  $0.001 \text{ dbar}$  (precision, not absolute accuracy), which corresponds to an accuracy of just under  $1 \text{ Sv}$  for the DWBC layer. The bottom pressure sensors can exhibit spurious drift trends that can lead to long-period pressure errors during the first few months of a deployment. However all pressure sensors used herein were dedrifted using the methods described by Watts and Kontoyiannis [1990] so any residual pressure drift errors should be less than  $0.015 \text{ dbar}$  and should be confined to the first few months of the record.

[7] The procedures described were applied to the first twelve months of daily PIES data to produce daily absolute velocity sections of the velocity component perpendicular to the PIES line. For the span between sites D and E (see Figure 1), a comparison between preliminary data from three lowered acoustic Doppler current profiler (LADCP) sections and the temporally-concurrent PIES-based transports indicated that the one-year-mean bottom-velocity was larger by about  $2 \text{ cm s}^{-1}$  (northward) than the mean of the historical current meters presented by Bryden et al. [2005a] so this correction was applied. No such correction was required at the other sites. Tidal signals were removed and all time series were subsequently smoothed with a seven-day Butterworth filter (2nd order) unless otherwise noted.

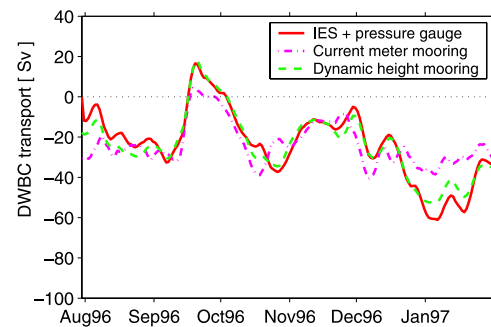


**Figure 2.** Transports integrated between sites B and D, 1200–4800 dbar, from an earlier pilot experiment. Figure illustrates the excellent agreement between the PIES transport estimates and the more traditional ‘picket fence’ current meter array. Also shown are the transport estimates using moored temperature sensors which have been combined with hydrography and bottom pressure data to produce a ‘dynamic height’ mooring. Units are Sverdrups ( $1 \text{ Sv} = 10^6 \text{ m}^3 \text{ s}^{-1}$ ). Figure adapted from Meinen et al. [2004].

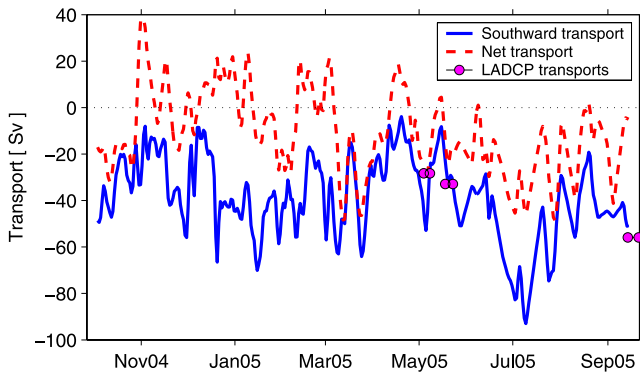


**Figure 3.** Absolute transports integrated between 800 and 4800 dbar and between the continental shelf and site E at 72°W after a 3-day lowpass filter. Both the integral of only the southward flow (blue solid line) and the integral of the net flow (red dashed line) are shown. Pairs of magenta dots, indicating the start and end time of the cruises, indicate the LADCP southward only transports integrated in the same manner as the PIES integration, while the distance between the dots indicates the time period over which the LADCP section was obtained. Units are Sverdrups ( $1 \text{ Sv} = 10^6 \text{ m}^3 \text{ s}^{-1}$ ).

Important note: as seen in Figure 1, there may be a non-trivial amount of the DWBC transport west of site B and below the depth of site A. This transport is estimated by assuming that the velocity structure inshore of B is similar to that between sites B and C.

### 3. Transport Results

[8] The volume transport time series obtained through these methods are shown in Figure 3. The time mean southward transport between the shelf and site E at 72°W integrated between 800 and 4800 dbar (the layer within which the DWBC is generally found) was 39 Sv ( $1 \text{ Sv} = 10^6 \text{ m}^3 \text{ s}^{-1}$ ). The statistical standard error of the mean is 4 Sv, and the standard deviation is 17 Sv. Variability is exhibited on all time scales from days to a few months (Figure 3), with southward transport values reaching up to 90 Sv. With only the first year of data available it is not yet possible to look at seasonal and longer time scales. Superimposed on this time series are the southward transport values estimated from the three snapshot LADCP sections, calculated by integrating the LADCP velocity profiles between the PIES sites in the same manner as for the PIES data (preliminary LADCP data provided by Lisa Beal via personal communication, 2006). The agreement between the two May 2005 sections and the PIES line is quite good, with the PIES transport time series essentially intersecting the LADCP

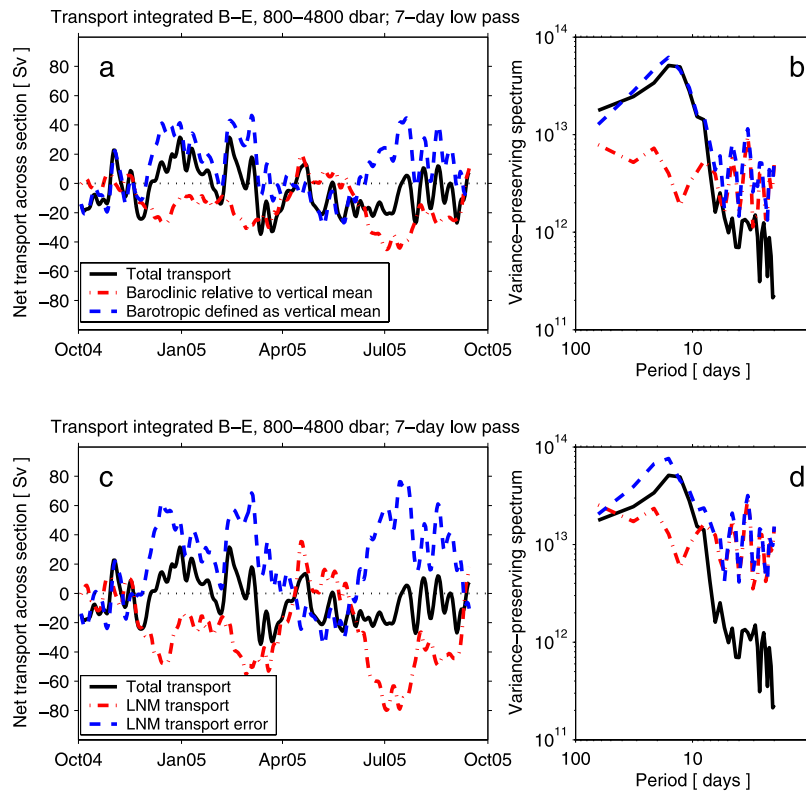


**Figure 4.** Transports integrated within 800–4800 dbar across the section between site B and site E. (a) Total, baroclinic, and barotropic components of the transport where the barotropic component is defined as the vertical mean over the full water column and the baroclinic velocity is defined relative to the vertical mean. (b) Variance preserving spectra of the time series shown in Figure 4a prior to the low-pass filtering. (c) Total, LNM transport, and LNM transport error where the LNM transport error is defined as the 800 dbar velocity multiplied by the layer thickness and the LNM transport is defined as relative to a LNM at 800 dbar. (d) Variance preserving spectra of the time series shown in Figure 4c prior to the low-pass filtering. Units for Figures 4a and 4c are Sverdrups.

transport values during the roughly 5–6 days it took to do each of the two LADCP sections. The September 2005 LADCP section was occupied September 14–21 while the PIES transport data is only available through September 14 when the first instrument data record was recovered. The September LADCP section has a transport that is roughly 5 Sv larger (to the south) than the final value of the PIES transport time series, however the PIES data are not truly coincident with the LADCP section. Overall the agreement between the LADCP and PIES transports is excellent, and lends confidence in both the PIES transport method overall and the basic method applied to estimate the transport inshore of PIES site B.

[9] Oceanic velocity measurements are often separated into barotropic (defined as the vertical mean over the full water column of the absolute velocity) and baroclinic (the variation relative to the vertical mean) components since the dynamics that control the two components are different. The transport of the DWBC can be separated into the contribution of these two velocity components; when this is done it becomes clear that the largest amplitude short period variability (<21 day) is in the barotropic component (e.g., a 40 Sv transition in less than a week in March 2005; see Figure 4a). The energy levels of the baroclinic and barotropic components, however, are very similar at periods shorter than 10 days with the exception of a tight band around 7–8 days where the barotropic energy is higher than the baroclinic (Figure 4b). The similarity of the energy levels between baroclinic and barotropic components at periods of 10 days and less, coupled with the fact that the total transport energy level is considerably lower at those frequencies, illustrates the compensation between baroclinic and barotropic components of the total transport. Note also that some of the baroclinic variations occur quite rapidly, with 10–20 Sv changes happening over a period of less than a week (e.g., late July 2005, see Figure 4a). This latter fact, coupled with the practical limitation that it takes on the order of 30 days to complete a trans-basin hydrographic section, is a concern. It has long been a tenet of physical oceanography that the majority of the time variability occurring over the course of a long section is barotropic in nature, and thus the baroclinic section was thought to be nearly “synoptic” even though it takes a month to complete. If 10–20 Sv baroclinic changes can occur during only a week this would imply much larger errors due to asynopticity in trans-basin sections in this area. Commonly these kinds of variations observed by an array that does not reach land at both ends would be ascribed to simple meandering of flows in-and-out at the end of the array; so-called “edge effects” of the array. However preliminary analysis of the PIES data in individual pairs (not shown) suggests that not all of the events observed in Figure 4a are obvious “edge effects” caused by flow motion in and out of the end of the PIES section at site E. More robust confirmation of this issue must wait for analysis of the PIES data in concert with the MOCHA-RAPID array stretching all the way across to the African continental shelf.

[10] Another concern that relates to hydrographic section transports becomes evident when the baroclinic and barotropic components are redefined in a way more consistent with how hydrographic data is often analyzed (Figure 4c). The standard hydrographic method generally defines the

baroclinic component relative to an assumed level of no motion (LNM) because the geostrophic method applied to hydrographic profiles provides only information about the velocity shear, i.e. the absolute velocity profile is indeterminate. In the region east of Abaco the 800 dbar level has commonly been chosen for a LNM based on long term current meter, LADCP, and Pegasus observations [Molinari *et al.*, 1992; Lee *et al.*, 1990, 1996; Hacker *et al.*, 1996; Bryden *et al.*, 2005a]. With the PIES data presented in this paper we can determine the DWBC transport relative to an 800 dbar LNM (‘LNM transport’) and the transport “error” incurred by assuming a LNM due to the actual motion at 800 dbar (‘LNM error’). The ‘LNM error’ is equal to the true 800 dbar velocity multiplied by the layer thickness. As is shown in Figure 4c, when an 800 dbar LNM is assumed the apparent variability of the DWBC (i.e. the ‘LNM transport’) is larger than that of the total transport and in particular is much larger than the ‘baroclinic’ transport variability shown in Figure 4a. The ‘LNM transport error’ is out of phase with the ‘LNM transport’ and largely mirrors the barotropic transports as shown in Figure 4a. For example, when the DWBC ‘LNM transport’ appears strong to the south, the velocity at 800 dbar is typically northward, reducing the total DWBC transport. Hence any sort of geostrophic-shear velocity time series estimate of the DWBC that does not use actual absolute velocity references may substantially overestimate the variability. In particular the amplitude increase of the LNM transport results in more short-period changes in the transport (e.g., an abrupt 30 Sv increase in southward LNM transport in June 2005). The spectra of the LNM transport and LNM error transport illustrate the increase in energy at all frequencies when the LNM assumption is made (compare Figures 4b and 4d). This occurs because at this location the baroclinic and barotropic variability are compensating for one another such that the intensity of the DWBC is inversely related to the flow at 800 dbar at essentially all frequencies. This result is not strongly dependent on the choice of LNM, and it illustrates the limitations of the LNM approach to estimating transports in this area.

#### 4. Discussion

[11] The total southward transport of  $39 \text{ Sv} \pm 4 \text{ Sv}$  (statistical standard error of the mean: SEM) to the south at  $26.5^\circ\text{N}$  is statistically indistinguishable from the  $40 \text{ Sv} \pm 3 \text{ Sv}$  (SEM) mean southward transport found in 1986–1992 by several ‘picket fence arrays’ of current meter moorings at roughly the same location [Lee *et al.*, 1990, 1996]. Bryden *et al.* [2005b], in an analysis of five trans-basin hydrographic sections at a nominal latitude of  $24^\circ\text{N}$  obtained between 1957 and 2004, found a decrease in the total basin-wide MOC transport of 30%, and this decrease occurred principally between 1992 and 2004. The majority of the upper limb of the MOC flow at this latitude is believed to be in the Florida Current, while the majority of the lower limb of the MOC is thought to be in the DWBC near the western side of the basin. There is no trend in the nearly-continuous Florida Current transport observations during the period from 1982 to the present (not shown), and the data presented herein suggest no indication of a trend in the DWBC transport over almost exactly the same time period as Bryden *et al.*

[2005b] between the current meter mean from 1986–1992 and the one-year PIES mean from 2004–2005. This may be because the one-year average from the PIES is insufficient to estimate the true modern mean, in which case future years of data should provide a better estimate of the signal in the western boundary area. Alternately this lack of signal near the western boundary of the basin may indicate that the signal observed by Bryden *et al.* [2005b] is occurring in the interior of the basin away from the western boundary. Future work will be required to determine why this signal does not appear in the western boundary region.

[12] As noted from the earlier mooring studies of Lee *et al.* [1990, 1996], much of the southward flow of the DWBC at 26.5°N recirculates to the north immediately to the east of the core of the southward flow and west of site E at 72°W (Figure 3). The time mean of the net transport between the continental slope and site E within the 800–4800 dbar layer (and including an estimate for the flow west of site B as discussed in the Methods section) is 11 Sv. The standard error of the mean is 4 Sv, and the standard deviation is 18 Sv. This southward through-flow for the DWBC transport is consistent with the transports observed upstream where the DWBC has been observed for several years by a current meter line just north of the Southeast Newfoundland Rise. At that location a mean southward flow of 12 Sv has been observed over the period 2000–2004 [Schott *et al.*, 2004]. Thus while the exact pathway of the DWBC flow from the exit of the subpolar gyre to the center of the subtropical gyre may not be clear, and recent float experiments suggest the DWBC may not simply “turn the corner” around the Southeast Newfoundland Rise [Fischer and Schott, 2002], by the time the flow reaches 26.5°N the transport at the base of the slope has the same magnitude as at the boundary of the subpolar gyre.

[13] In summary, the first year of data from the NOAA 26.5°N PIES monitoring line demonstrates high variability in both the barotropic and baroclinic components of the DWBC transport integrated between 800 and 4800 dbar and between the continental shelf and 72°W. Baroclinic (defined as the velocity variations relative to the vertical mean) and barotropic transport energy levels are very similar at periods less than 10 days, while the barotropic energy levels are higher at periods of 10–80 days. Applying an assumption for a level of no motion artificially increases the apparent energy levels in the velocity component relative to the level of no motion at all observed frequencies. The 1-year-mean southward transport of 39 Sv is statistically indistinguishable from the 40 Sv estimate obtained at the same location by current meter mooring arrays in the late 1980s and early 1990s.

[14] **Acknowledgments.** The authors would like to express our thanks to Bill Johns for providing some of the ship time needed to maintain the IES array and to Lisa Beal for providing the preliminary LADCP data used herein. Rick Lumpkin and two anonymous reviewers made several suggestions for improving the manuscript. Thanks also to the following contributors to the program in 2004–2005: David Bitterman, Tania Casal, Guilherme Castela, Carlos Fonseca, Rigoberto Garcia, Mark Graham, Humberto Guarin, Ben Kates, Robert Jones, Jon Molina, Dallas Murphy, Brad Parks, Ulises Rivero, Robert Roddy, Deb Shoosmith, Xiaobiao Xu, and the officers and crews of the NOAA Ship Ronald H. Brown and the R/V Knorr. The Western Boundary Time Series program is funded by the NOAA Office of Climate Observations.

## References

- Baehr, J., J. Hirschi, J. Beismann, and J. Marotzke (2004), Monitoring the meridional overturning circulation in the North Atlantic: A model-based array design study, *J. Mar. Res.*, *62*(3), 283–312, doi:10.1357/0022240041446191.
- Baringer, M. O., and J. C. Larsen (2001), Sixteen years of Florida Current transport at 27°N, *Geophys. Res. Lett.*, *28*(16), 3179–3182.
- Bryden, H. L., W. E. Johns, and P. M. Saunders (2005a), Deep Western Boundary Current east of Abaco: Mean structure and transport, *J. Mar. Res.*, *63*, 35–57.
- Bryden, H. L., H. R. Longworth, and S. A. Cunningham (2005b), Slowing of the Atlantic meridional overturning circulation at 25°N, *Nature*, *438*, 655–657.
- Fischer, J., and F. A. Schott (2002), Labrador Sea water tracked by profiling floats: From the boundary current into the open North Atlantic, *J. Phys. Oceanogr.*, *32*(2), 573–584.
- Hacker, P., E. Firing, W. D. Wilson, and R. Molinari (1996), Direct observations of the current structure east of the Bahamas, *Geophys. Res. Lett.*, *23*(10), 1127–1130.
- Hirschi, J., J. Baehr, J. Marotzke, J. Stark, S. A. Cunningham, and J.-O. Beismann (2003), A monitoring design for the Atlantic meridional overturning circulation, *Geophys. Res. Lett.*, *30*(7), 1413, doi:10.1029/2002GL016776.
- Johns, W. E., T. Kanzow, and R. Zantopp (2005), Estimating ocean transports with dynamic height moorings: An application in the Atlantic Deep Western Boundary Current, *Deep Sea Res., Part I*, *52*(8), 1542–1567, doi:10.1016/j.dsr.2005.02.002.
- Larsen, J. C. (1992), Transport and heat flux of the Florida Current at 27°N derived from cross-stream voltages and profiling data: Theory and observations, *Philos. Trans. R. Soc. London, Ser. A*, *338*, 169–236.
- Larsen, J. C., and T. B. Sanford (1985), Florida Current volume transports from voltage measurements, *Science*, *227*(4684), 302–304.
- Lee, T. N., W. Johns, F. Schott, and R. Zantopp (1990), Western Boundary Current structure and variability east of Abaco, Bahamas at 26.5°N, *J. Phys. Oceanogr.*, *20*(3), 446–466.
- Lee, T. N., W. E. Johns, R. J. Zantopp, and E. R. Fillenbaum (1996), Moored observations of Western Boundary Current variability and thermohaline circulation at 26.5°N in the subtropical North Atlantic, *J. Phys. Oceanogr.*, *26*(6), 962–983.
- Meinen, C. S., and D. R. Watts (2000), Vertical structure and transport on a transect across the North Atlantic Current near 42°N: Time series and mean, *J. Geophys. Res.*, *105*(C9), 21,869–21,892.
- Meinen, C. S., S. L. Garzoli, W. E. Johns, and M. O. Baringer (2004), Transport variability of the Deep Western Boundary Current and the Antilles Current off Abaco Island, Bahamas, *Deep Sea Res., Part I*, *51*, 1397–1415.
- Molinari, R. L., R. A. Fine, and E. Johns (1992), The Deep Western Boundary Current in the tropical North Atlantic Ocean, *Deep Sea Res.*, *39*(11), 1967–1984.
- Schott, F. A., R. Zantopp, L. Stramma, M. Dengler, J. Fischer, and M. Wibaux (2004), Circulation and deep-water export at the western exit of the subpolar North Atlantic, *J. Phys. Oceanogr.*, *34*(4), 817–843.
- Srokosz, M. A. (2003), Rapid climate change: Scientific challenges and the new NERC programme, *Philos. Trans. R. Soc. London, Ser. A*, *361*, 2061–2078, doi:10.1098/rsta.2003.1243.
- Stouffer, R. J., J. Yin, and J. M. Gregory (2006), Investigating the causes of the response of the thermohaline circulation to past and future climate changes, *J. Clim.*, *19*(8), 1365–1387.
- Vellinga, M., and R. A. Wood (2002), Global climatic impacts of a collapse of the Atlantic thermohaline circulation, *Clim. Change*, *54*(3), 251–267.
- Watts, D. R., and H. Kontoyiannis (1990), Deep-ocean bottom pressure measurement: Drift removal and performance, *J. Atmos. Oceanic Technol.*, *7*(2), 296–306.
- Watts, D. R., C. Sun, and S. Rintoul (2001a), A two-dimensional gravest empirical mode determined from hydrographic observations in the subantarctic front, *J. Phys. Oceanogr.*, *31*(8), 2186–2209.
- Watts, D. R., X. Qian, and K. L. Tracey (2001b), Mapping abyssal current and pressure fields under the meandering Gulf Stream, *J. Atmos. Oceanic Technol.*, *18*(6), 1052–1067.

M. O. Baringer, S. L. Garzoli, and C. S. Meinen, Physical Oceanography Division, Atlantic Oceanographic and Meteorological Laboratory, 4301 Rickenbacker Causeway, Miami, FL 33149, USA. (christopher.meinen@noaa.gov)